

# Optimal Operation of a Photovoltaic Induction Motor Drive Water Pumping System

Nelson K. Lujara

**Abstract**—The performance characteristics of a photovoltaic induction motor drive water pumping system with and without maximum power tracker is analyzed and presented. The analysis is done through determination and assessment of critical loss components in the system using computer aided design (CAD) tools for optimal operation of the system. The results can be used to formulate a well-calibrated computer aided design package of photovoltaic water pumping systems based on the induction motor drive. The results allow the design engineer to pre-determine the flow rate and efficiency of the system to suit particular application.

**Keywords**—Photovoltaic, water pumping, losses, induction motor.

## I. INTRODUCTION

THE use of photovoltaic water pumping systems has recently received increasing attention especially in areas where solar energy is abundant and in remote areas where grid power is either not feasible or non-existent. More than a decade ago there were more than 50,000 PV water-pumping systems around the world and the number has been steadily increasing [1].

The simplest and least expensive method in a photovoltaic system is to connect the load directly to a photovoltaic generator (without storage batteries). Such installations are referred to as direct-coupled systems and have several advantages over PV systems with battery back-up systems or utility grid connected systems [2], [3].

Direct-coupled systems are normally fitted with maximum power trackers (MPT) connected between the PV array and the load to improve the performance of the system. The MPT, usually a dc-dc converter is used to force the PV array to operate at its maximum power point regardless of the load, insolation or temperature changes.

In this paper the losses in a direct-coupled PV induction motor (IM) drive water pumping system is analyzed from the point of view of optimizing the system performance taking into account the variations in the system head. Losses are a major design criterion in photovoltaic water pumping systems primarily because the size and the cost of the generator, which accounts for the largest portion of the cost of the system is dependent on the losses of the system [4].

## II. SYSTEM ARRANGEMENT

The system consisted of a set of PV modules rated 200 V connected to a 100-V PWM inverter supplying a 2-pole three-phase induction motor rated 200 V, 60 Hz, 2.8 A. The motor was mechanically coupled to the pump using a pulley of ratio 1:2. In the other arrangement, depending on the output of the PV array buck and boost converters were interfaced between the array and the inverter in succession in order to optimize the performance of the system due to the insolation variations.

### A. Induction Motor

#### 1. Stator Copper Losses

Stator copper losses were determined from;

$$P_s = k \cdot I_{rms}^2 \cdot R_1 \quad (1)$$

where;  $k$  = number of phases,  $R_1$  = the stator resistance,  $I_{rms}$  = rms current flowing in the motor.

#### 2. Rotor Copper Losses

Fig. 1 shows the waveform of the motor input current when the motor is driving the pump at a frequency of 10 Hz with the motor supplied from a PWM inverter. The waveform contains harmonics at higher frequency only. Since harmonic currents at low frequency are absent, the harmonic rotor copper losses were neglected.

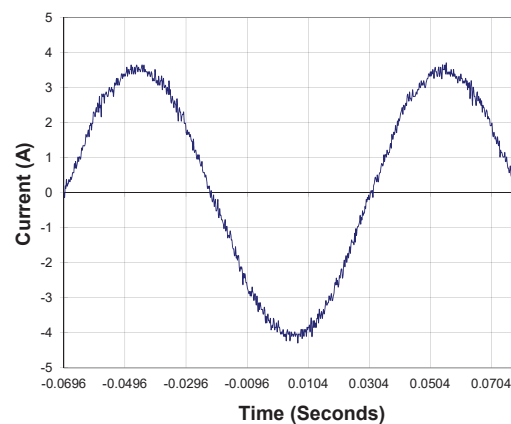


Fig. 1 The motor input current

The rotor copper loss for the fundamental field is evaluated using (2) as [5];

$$P_r = T_e \cdot (\omega_s - \omega_m) = T_e \cdot s \cdot \omega_s \quad (2)$$

N. K. Lujara is with the Department of Electrical Engineering, College of Engineering and Technology, University of Dar es Salaam, P. O. Box 35131, Tanzania (phone: +255 754 554 403, e-mail: nklujara@gmail.com).

where,  $s$  = Slip,  $\omega_m$  = Rotor speed (rad/sec),  $\omega_s$  = Synchronous speed (rad/sec).

The electromagnetic torque,  $T_e$  is obtained from the air-gap power,  $P_g$  obtained from the motor power input and the stator losses, i.e.

$$P_g = T_e \cdot \omega_s = P_{in} - P_s \quad (3)$$

where;  $P_{in}$  = Motor input power,  $P_s$  = Stator copper losses.

### 3. Core Losses

Core losses were also evaluated at fundamental frequency as,

$$P_c = k \cdot I_c^2 \cdot R_c \quad (4)$$

where,  $I_c$  = rms current in the core,  $R_c$  = Core resistance.

### 4. Mechanical Losses

Mechanical losses were determined by directly coupling the motor to an auxiliary drive. The coupling was implemented using a hard rubber coupling whose losses were assumed to be negligible. The resulting mechanical losses as a function of speed are shown in Fig. 2. The kink in Fig. 2 was due to mechanical vibration of the system. That part of the graph was ignored in subsequent computations.

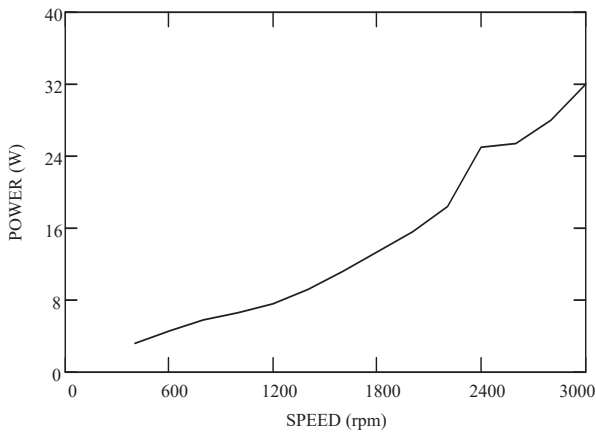


Fig. 2 Mechanical losses of the induction motor

### 5. Stray Load Losses

Stray load losses were estimated to be 1% of the full-load power output [6]; thus

$$P_s = 0.01 \cdot \sqrt{3} \cdot V_L \cdot I_L \cdot \cos\phi \quad (5)$$

where;  $V_L$  = Line-to-line rated voltage,  $I_L$  = Line-to-line rated current,  $\cos\phi$  = Power factor at rated load.

## B. Inverter

A PWM voltage source inverter has been used in the analysis and experiment. The analysis involved the determination of the conduction and switching losses in the MOSFETs which were used as switching devices. The calculation of losses in the freewheeling diode has been covered in [7], this work has therefore adopted this analysis taking into account the number of devices used in the inverter.

### 1. Conduction Losses

Conduction losses in one MOSFET of the inverter are determined as shown in (6):

$$P_c = I_{rms}^2 \cdot R_{DS(on)} \quad (6)$$

where,  $I_{rms}$  = rms current flowing in the switch,  $R_{DS(on)}$  = Drain-to-source resistance at a junction temperature

The currents in (6) involve the determination of the rms and the average values of the device currents. These currents are calculated by determining the current due to each pair of voltage pulses and notches and then the effect of all pulses and notches are combined to obtain the effective currents. This work has been successfully analysed in [7].

### 2. Switching Losses

The switching losses are generally obtained from;

$$P_s = f_s \cdot \int_0^{t_s} v(t) \cdot i(t) dt \quad (7)$$

where,  $f_s$  = Switching frequency,  $t_s$  = Switching time,  $v(t)$  = Time dependent voltage in the switch,  $i(t)$  = Time dependent current in the switch,

The device currents in (7) is obtained by first establishing the current that flows in each pulse of the load current in one leg of the PWM inverter. The current, which is a series of pulses, can be obtained if the switching instants, the pulse and notch width are known [6].

## III. SIMULATION RESULTS

### A. The IM Drive without MPT

Fig. 3 shows the efficiency of the PV array. The control of the inverter output power is done by the variation of the modulation index. The control of the modulation index maintains constant inverter input power while supplying the load with the required voltage. Since at a given insolation the array input power is also constant, the array efficiency remains constant throughout the operating head.

### 1. Motor

The motor losses are shown in Fig. 4. The losses in the stator are high due to the high stator resistance of the motor. Since stator losses are dominant, the characteristic curve of the total losses resembles that of the stator losses. The stator losses increase as the head is increased since the torque

demand is also increased, thus decreasing the efficiency of the motor as shown in Fig. 5.

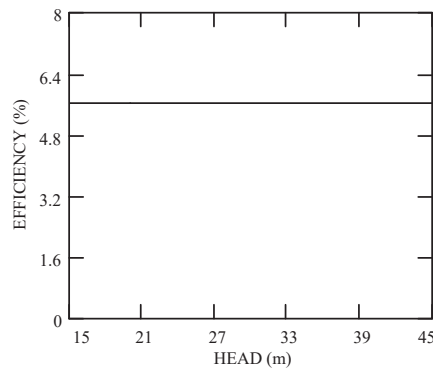


Fig. 3 Array efficiency at constant reference insolation

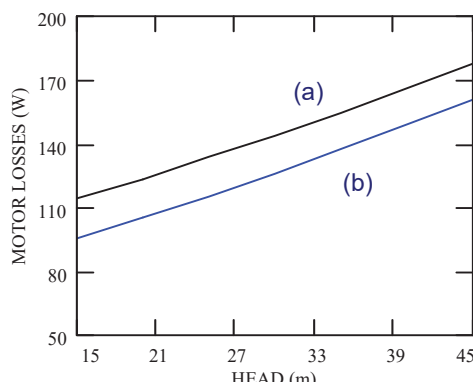


Fig. 4 Motor losses (a) Total losses (b) Stator losses

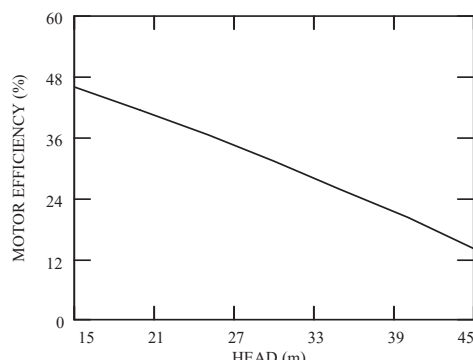


Fig. 5 Motor efficiency

## 2. Inverter

The major losses in the MOSFET based PWM inverter are conduction losses. These losses depend on the load current. The current flowing in the switches and freewheeling diodes increases due to the increase in the stator current as the head is increased. Figs. 6 and 7 show inverter losses and efficiency at a switching frequency of 10 kHz, respectively. The losses vary between 10.3 W at a head of 15 metres to 14.6 W at a head of 45 metres giving efficiencies above 93% for the whole range of operating head.

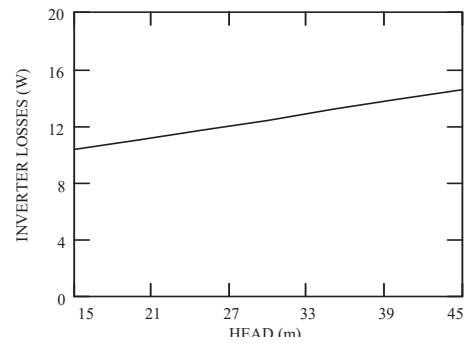


Fig. 6 Inverter losses

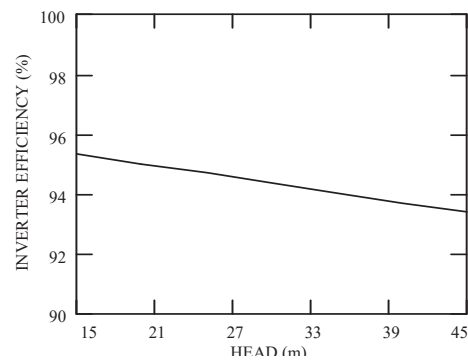


Fig. 7 Inverter efficiency

## B. The IM Drive with MPT

The array operating point at constant insolation is constant when a maximum power tracker is included in the system. With the input and output power constant, the efficiency of the array against the head remains constant. The losses, duty cycle and efficiency of the MPT also remain unchanged. The motor stator voltage required to develop the required torque at different heads is obtained by varying the modulation index.

### 1. Inverter

Inverter losses and efficiency are shown in Figs. 8 and 9, respectively. The voltage and frequency variation in the operating plane of the inverter when the head is varied from 15 metres to 45 metres is the same as in the system without a MPT. There is a negligible change in the inverter output current (and therefore negligible change in the device currents) when a MPT is included in the system, because the change in the stator voltage and impedance of the motor is very small. For this reason, there is no significant change in the losses and efficiencies of the system with or without a maximum power tracker. The maximum difference between the losses and efficiencies for the two systems do not exceed 0.9% and 0.6%, respectively.

### 2. Motor

Fig. 10 shows the losses of the PWM inverter-fed induction motor. There is no significant change in the losses of the motor when a maximum power tracker is included in the system. The stator losses, which are the major loss in the motor, vary between 95.6 W and 160.6 W when the head is

varied from 15 m to 45 m in the system without MPT (Fig. 4). These losses vary between 96.4 W and 161.5 W when a MPT is used in the same range of head (Fig. 10).

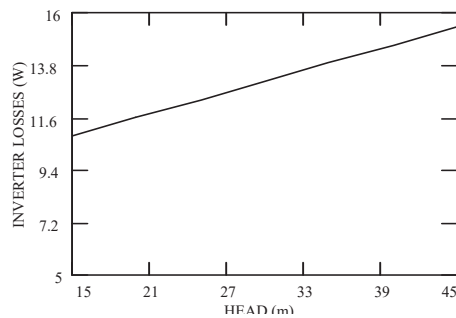


Fig. 8 Inverter losses

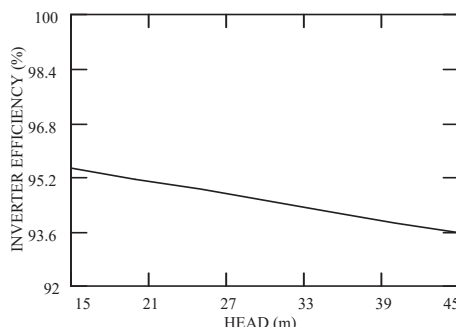


Fig. 9 Inverter efficiency

The efficiency of the motor is shown in Fig. 11. The efficiency is 49% and 20% at a head of 15 and 45 metres, respectively as compared to efficiencies of 46% and 13% at the same heads for the system without a maximum power tracker.

## V. EXPERIMENTAL VALIDATION

The comparison between the measured and the simulated results of the systems with and without maximum power tracker is tabulated in Tables I and II respectively. The

experimental values in both systems have shown good correspondence with the computed results within a 10% error margin in all parameters. The simulation models developed have therefore been shown to be accurate. Explanation for the marginal differences between the measured and computed results in some cases have been provided and shown to be mainly due to accuracy limits of the measuring instruments used

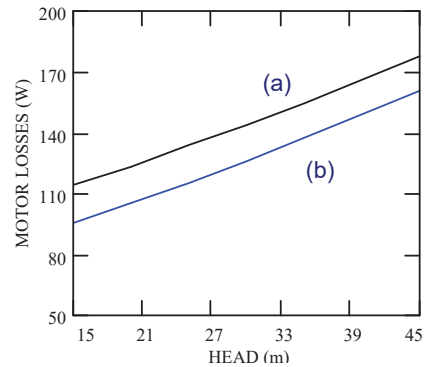


Fig. 10 Motor losses (a) Total losses (b) Stator losses

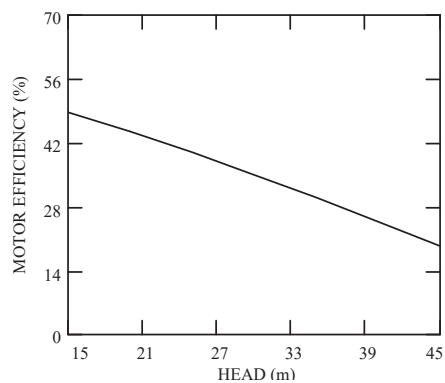


Fig. 11 Motor efficiency

TABLE I  
SIMULATION AND EXPERIMENTAL RESULTS OF IM DRIVE WPS WITHOUT MPT

H	Inverter losses			Motor losses			Flow rate			Motor speed		
	$P_{i_s}$	$P_{i_e}$	% er	$P_{m_s}$	$P_{m_e}$	% er	$Q_s$	$Q_e$	% er	$n_s$	$n_e$	% er
15	10.797	11	1.85	114.39	120	4.6	329.5	330	-1.4	1080	1077	-0.28
20	11.53	12.5	7.8	123.62	126	1.9	278.24	270	-3.1	912	908	-0.44
25	12.277	13.2	7	133.55	139	3.9	231.87	225	-3.1	760	759	-0.13
30	13.034	14.2	8.2	143.91	146	1.4	189.16	180	-5.1	620	619	-0.16
35	13.787	14.8	6.8	154.59	160	3.4	146.44	140	-4.6	480	480	0
40	14.543	15.5	6.2	166.06	172	3.5	108.61	105	-3.4	356	354	-0.56
45	15.29	17	10	178.02	186	4.3	71.7	68	-4.6	235	233	-0.86

H = Pumping height in metres,  $P_{m_s}$  = Simulated motor losses (W),  $P_{m_e}$  = Measured motor losses(W),  $P_{i_s}$  = Simulated inverter losses (W),  $P_{i_e}$  = Measured inverter losses (W),  $Q_s$  = Simulated flow rate(l/h),  $Q_e$  = Measured flow rate (l/h),  $n_s$  = Simulated Speed (rpm),  $n_e$ = measured speed (rpm), %er= % error =  $\frac{\text{Measuredvalue}-\text{Simulatedvalue}}{\text{Measuredvalue}}$

TABLE II  
SIMULATION AND EXPERIMENTAL RESULTS OF THE IM DRIVE WITH MPT

MPT losses				Inverter losses			Motor losses			Flow rate		
$H$	$P_{p_s}$	$P_{p_e}$	% $er$	$P_{i_s}$	$P_{i_e}$	% $er$	$P_{m_s}$	$P_{m_e}$	% $er$	$Q_s$	$Q_e$	% $er$
15	1.37	1.5	8.6	10.842	11.2	3.2	114.21	120	4.8	381.36	375	-1.7
20	1.37	1.4	2.1	11.583	12.7	8.8	122.52	126	2.8	332.55	325	-2.3
25	1.37	1.5	8.6	12.334	13.5	8.6	131.67	136	3.2	281.29	275	-2.3
30	1.37	1.4	2.1	13.103	14.2	7.7	141.66	145	2.3	236.44	230	-2.8
35	1.37	1.4	2.1	13.876	14.8	6.2	151.99	158	3.8	192.21	190	-1.2
40	1.37	1.4	2.1	14.65	15.8	7.3	162.73	170	4.3	151.02	150	-0.68
45	1.37	1.4	2.1	15.423	17	9.3	174.16	180	3.2	112.27	110	-2.1

$P_{p_e}$ = Simulated MPT losses (W),  $P_{p_e}$ = Measured MPT losses (W)

## VI. CONCLUSION

The work in this paper has analyzed the critical loss components in PV induction motor drive water pumping system. The accuracy of the developed model has been shown by the good correspondence between the simulated and experimental results. The algorithms developed therefore have provided groundwork for a computer aided design (CAD) tool for optimal design of PV water pumping systems based on induction motor drive. The CAD tool would enable the establishment of the optimal operation of a system for a particular application.

## REFERENCES

- [1] The World Directory of Renewable Energy, Suppliers and Services 1995, James & James Science Publishers Ltd. 110-156.
- [2] Hsiao, Y. R, Blevens, B.A. Direct Coupling of photovoltaic power source to water Pumping System "Solar Energy, Vol.32, 1984, pp 489-498.
- [3] N.K. Lujara, "Computer Aided Modelling of Systems for Solar Powered Water Pumping by Photovoltaic" D.Ing thesis, Rand Afrikaans, University, March 1999, Ch 1, 1-20, Ch 2, 21-62.
- [4] N.K. Lujara, "Loss Characteristics of Permanent Magnet DC Motor Drive Water Pumping Systems" Tanzania Journal of Engineering and Technology (TJET), Vol.5 No. 2, November 2014, pp 79-88.
- [5] J.D. van Wyk, "Electronic Control of Electromechanical Energy Conversion in Electrical Machines "Ph.D. thesis, Technical University of Eindhoven, August 1969, 56-58.
- [6] J.M.D Murphy, V.B. Hosinger, "Efficiency Optimization of Inverter-Fed Induction Motor Drives" Conf. Record IEEE-IAS 1982 Annual meeting, 544-552.
- [7] Nelson K. Lujara, "Three phase PWM Inverter for Low Rating Energy Efficient Systems" International Journal of Electrical, Computer, Electronics and Communication Engineering, Vol. 9 No. 4, 2015, pp 400-406.